Proc. Natl. Acad. Sci. USA
Vol. 76, No. 12, pp. 6132–6136, December 1979
Biochemistry

Electron-nuclear double resonance of the hydrogen peroxide compound of cytochrome *c* peroxidase: Identification of the free radical site with a methionyl cluster

(electron paramagnetic resonance)

BRIAN M. HOFFMAN, JAMES E. ROBERTS, THEODORE G. BROWN*, CHAE HEE KANG, AND E. MARGOLIASH

Departments of Chemistry and of Biochemistry and Molecular Biology, Northwestern University, Evanston, Illinois 60201

Contributed by Emanuel Margoliash, September 4, 1979

ABSTRACT **The results of electron-nuclear double resonance and electron paramagnetic resonance (EPR) studies on the hydrogen peroxide compound of yeast cytochrome *c* peroxidase are inconsistent with previous proposals for the source of the EPR signal in this compound, in particular with its identification with an aromatic amino acid radical such as would arise by oxidation of a tryptophanyl side chain. The present observations lead us to propose that the EPR signal is associated with a cluster containing at least one methionine and in which proximate side chains share the charge created by loss of one electron.**

Yeast cytochrome *c* peroxidase reacts with hydrogen peroxide to produce an enzymatically active compound that has been oxidized two equivalents above the ferriheme resting state (1–4); this compound has been called ES by Yonetani (2). ES is at the same level of oxidation as compound I of horseradish peroxidase and of catalase (5) but is quite unlike them in several respects. It is remarkably stable (4); optical spectra (2), Mössbauer spectra (6), and static susceptibility measurements (7) indicate that it contains an $S = 1$, Fe(IV) heme and a species with $S = 1/2$; it exhibits an intense electron paramagnetic resonance (EPR) signal (8, 9).

The source of the EPR signal has been a matter of substantial interest for well over a decade. The first suggestion was that one of the two oxidizing equivalents in ES exists as a stable free radical of an aromatic amino acid (8). In support of this concept, the amino acid composition of ES decay products can be interpreted as implicating tryptophan or tyrosine (10), and recent x-ray diffraction studies have demonstrated the presence of a tryptophan adjacent to the heme (11). Another early suggestion was that ES contained a heme-bound peroxy radical (12).

We here report EPR and electron-nuclear double resonance (ENDOR) (13, 14) measurements of ES. The results appear to exclude any of the previous suggestions for the source of the ES EPR signal. Instead, we propose that the EPR signal is sulfur-based and involves methionine. The best available model is a dimeric thioether radical cation $(R_2SSR_2)^+$ in which two proximate methionyl side chains share the charge created by the loss of one electron.

EXPERIMENTAL

Baker's yeast cytochrome *c* peroxidase was prepared as described (15). Samples of ES were prepared from the enzyme in its ferric state (≈1.5 mM) in 10 mM sodium acetate buffer (pH 6.0) by addition of H_2O_2 in slight stoichiometric excess. They were then rapidly frozen and stored at 77 K.

ENDOR experiments were performed below the λ point of liquid helium by immersing the microwave cavity in a bath of superfluid helium. The ENDOR spectrometer, which uses 100-KHz detection, is described elsewhere (16). Typical conditions were microwave power of ≈6 mW, field-modulation amplitude of 3–4 G, and radiofrequency field of ≈1 G in the rotating frame. Simulated EPR spectra were calculated by using program SIM 14 (Quantum Chemistry Program Exchange, no. 265); ENDOR simulations will be described elsewhere (unpublished). Molecular orbital calculations utilized a program (A. L. Allred and D. Larsen, personal communication) implementing the Hückel–McLachlan technique (17).

EPR Spectra of the Hydrogen Peroxide Compound of Cytochrome *c* Peroxidase. *Observation.* Fig. 1 presents the standard absorption mode-derivative EPR signal of ES and the dispersion-mode derivative signal under high microwave power, both taken at 2 K. The signal, which is stoichiometric with the heme (8, 9), is characteristic of a $S = 1/2$ species with axial g-tensor, $g_\parallel = g_z = 2.05$, $g_\perp = g_x = g_y = 2.01$.

On computer simulation of the 2 K signal using these g values, a component Gaussian line, and a linewidth tensor of $W_\parallel = 35$ G and $W_\perp = 20$ G gives a good fit to the parallel region, but the signal in the perpendicular region has a broader "tail" than predicted. The best overall fit is obtained with a Lorentzian component line with $W_\parallel = 28$ G and $W_\perp = 15$ G (Fig. 1), suggesting that the resonance is homogenously broadened by spin-relaxation—for example, by exchange interactions with the heme. However, ENDOR is observed under saturating conditions (see below), indicating inhomogeneous broadening (13, 18). Thus, the shape of the spectrum more likely results from unresolved hyperfine splitting (hfs) or the distribution in $g_\parallel$ values and hfs values which is suggested below, or both. Inhomogeneous broadening requires the individual component linewidth to be much less than the simulation widths. This, in turn, suggests that dipolar broadening by the heme is small and that the radical is removed from the heme iron, as suggested earlier (9).

The absorption mode signal at 1.4 K has been reported to be somewhat variable in shape, depending on the oxidant (9). We have examined only the H_2O_2-oxidized protein and find the 2 K spectrum to be independent of the buffer anion. Although the 77 K signal is not isotropic, as originally reported (8), it appears to broaden in the $g_\parallel$ region or shift, depending on the medium. This could occur if there is a temperature-dependent conformational equilibrium that produces a temperature-dependent distribution in $g_\parallel$ values and if this equilibrium is sensitive to the environment.

The publication costs of this article were defrayed in part by page charge payment. This article must therefore be hereby marked "*advertisement*" in accordance with 18 U. S. C. §1734 solely to indicate this fact.

Abbreviations: ENDOR, electron-nuclear double resonance; EPR, electron paramagnetic resonance; ES, hydrogen-peroxide compound of yeast cytochrome *c* peroxidase; hfs, hyperfine splitting.

* Present address: Department of Chemistry, University of California, Davis, CA 95616.

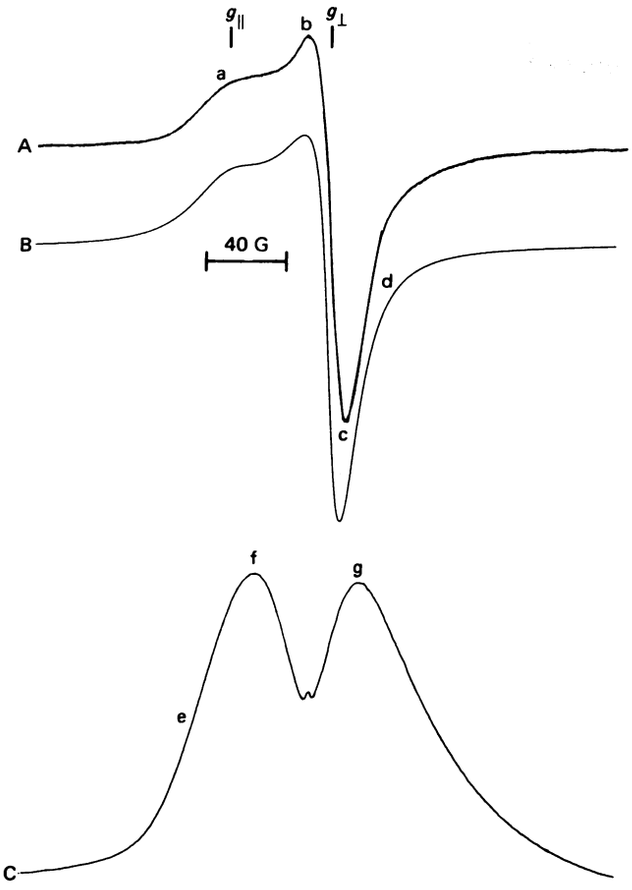

FIG. 1. EPR spectra of ES at 2 K. Curves: A, absorption mode-derivative spectrum at low microwave power (50 dB; 2 μW); B, computer simulation using g-values and lineshape parameters given in the text; C, dispersion-mode derivative spectrum taken under saturating conditions (15 dB, 6 mW). Field positions marked by letters a to g are those for which ENDOR is discussed.

The EPR spectrum cannot be saturated at 77 K with the available X-band microwave power (≈200 mW). At 2 K, microwave saturation, as indicated by a "knee" in the curve of the signal height vs. microwave field, can be achieved but only at relatively high powers (≈15 dB; ≈6 mW). The spin-lattice relaxation time varies across the spectrum, with the $g_\perp$ region saturating more readily than the $g_\parallel$, indicating that cross relaxation is slow and justifying the description of the magnetic field variation of the ENDOR spectrum given below.

As originally noted by Yonetani *et al.* (8), the ES g-shifts ($\delta g_i \equiv g_i - g_e$) from the free-electron value (g_e) are too small to arise from a species involving the heme iron. The temperature-independent magnetic moment (77–300 K) (7) and EPR spin quantitation at 1.4 K (9) and at 77 K (8), the observed g values, and the Mössbauer measurements (6), in combination with our observation of inhomogeneous broadening and a signal shape that is only modestly temperature dependent, show that the resonance is not associated with the $S = 1/2$ state resulting from exchange-coupling between the $S = 1$ heme iron and a free radical, whether the latter is on the porphyrin or on an amino acid side chain. Thus, the EPR signal of ES arises from an independent $S = 1/2$ species.

Analysis. The characteristics of the ES EPR signal do not support an identification with the aromatic π-electron free radical of a tyrosyl, histidyl, or tryptophanyl residue. First, as noted earlier, the g shifts are too large for such a radical (9). Phenoxy radicals normally have g shifts much smaller than that of ES, with $|\delta g_i| < 0.01$ for all $i = x,y,z$ (19); the tyrosyl radical, either neutral or ionized, is not reported to have an unusual anisotropy (20). Nitrogen heterocycle radicals likewise have the typically small π-radical g shifts, $|\delta g_i| < 0.01$ (21). Moreover, one expects $|\delta g_\perp| > |\delta g_\parallel| \approx 0$ for a planar π radical, contrary to observation for ES (22). Finally, through calulations such as those of Schulz *et al.* (23) one may show that spin-coupling between the $S = 1$ heme and a radical cannot produce the observed g values. The g values of ES are consistent with those of a peroxy radical (12). However, studies with various oxidants make it unlikely that a peroxy fragment is retained in ES (24).

The above conclusions have led us to consider sulfur-based radicals. Most of the sulfur radicals that might occur in a protein have chemical and physical properties inconsistent with those of ES. The ES g shifts are far too small to be associated with the monovalent sulfur of a cysteinyl radical, for which representative g values are 2.2441, 2.0006, and 1.9837 (25). Furthermore, it has been shown that the EPR signal of ES is formed quantitatively despite p-chloromercuribenzoate blockage of the single cysteine of cytochrome c peroxidase (unpublished). This experiment also rules out a radical of the form $RSSR_2$, such as would arise from the dimerization of a cysteinyl radical and a methionyl residue. In addition, the enzyme has no disulfide linkages (4), excluding a disulfide cation radical. Thioether cation radicals, in the form of a dimer $(R_2SSR_2)^+$ (26, 27) or interacting with a nitrogenous nucleophile $(R_2SNR_3)^+$ (28), are well-characterized species exhibiting g shifts comparable to those of ES. Sites involving methionyl cation radicals are discussed in detail in the analysis of the ENDOR results.

Basis for Analysis of Protein ENDOR Spectra. ENDOR is performed by inducing nuclear transitions with a radiofrequency field while keeping the static magnetic field, H_0, set at a fixed value. When cross relaxation is slow, as in ES, the ENDOR signal arises from that subset of molecules with orientations such that EPR occurs in the vicinity of H_0 (29). Field positions in the "parallel region" (positions a and e in Fig. 1) will give single crystal-like spectra that arise from free-radical centers with H_0 along $g_\parallel$. Computer calculations using the g and linewidth tensors for ES indicate that the signal at field position f on the spectrum in Fig. 1 also arises in large part from these same centers ($H_0 \parallel g_\parallel$); thus position f will also be denoted as a parallel field. In contrast, positions c, d, and g in the "perpendicular" region of the EPR spectrum give rise to an ENDOR pattern that is essentially a superposition from molecules with H_0 lying in the plane normal to $g_\parallel$.

ENDOR signals from ES might in principle be associated with ^1H or ^{14}N. In a protein having a particular orientation, $\Omega = (\theta,\phi)$ with respect to H_0, the normal ENDOR pattern for a set of magnetically equivalent protons is a pair of lines with frequencies $\nu^H(\Omega)$ which are mirrored about the free-proton frequency, $\nu_p = g_H\beta_n/hH_0$ (13.62 MHz at 3200 G) (13, 14):

$$\nu^H(\Omega) = \nu_p \pm A^H(\Omega)/2. \qquad [1]$$

The two values of ν^H are split by the angle-dependent hyperfine coupling, $A^H(\Omega)$, which is written in terms of the hfs tensor principal axis a values (A_1^H, A_2^H, A_3^H) and the g values (13). For a frozen solution the signal intensity in an ENDOR spectrum typically shows discernible features at frequencies corresponding to the hfs tensor principal axis values [where $A^H(\Omega) \approx A_i^H$ (29)]. Because ν_p varies in proportion to the microwave frequency, when the magnetic field is set to correspond to a given position on the EPR spectrum (e.g., a in curve A of Fig.

1), the center of a proton ENDOR pair also varies in this fashion. However, the splitting A^H is independent of microwave frequency.

A single set of equivalent ^{14}N nuclei normally exhibits a four-line ENDOR pattern centered at $A^N(\Omega)/2$ (13). In contrast to proton ENDOR signals, the center position of the ^{14}N pattern is independent of microwave frequency.

ENDOR of the Hydrogen Peroxide Compound of Cytochrome *c* Peroxidase. *Observation.* ENDOR of ES was observed as a decrease in the EPR signal with the EPR spectrometer tuned to either the absorption or dispersion mode. The dispersion mode was ordinarily used because better signals are obtained and the uninformative "matrix" ENDOR peak center at ν_p is suppressed (30). ENDOR spectra were recorded at the fields labeled a to d in Fig. 1 with the EPR absorption mode and fields e to g with dispersion, with the ENDOR signal strength scaling as the EPR signal.

Curves A and B of Fig. 2 display ENDOR absorption spectra (2 K) taken over a range of ≈2 to 30 MHz in the dispersion mode at a parallel field position (f) and at a perpendicular field position (g). No other signals were observed at any field position up to frequencies of ≈100 MHz. Better resolution, albeit with lower signal-to-noise ratio, was obtained from the derivative presentation (curves C to E in Fig. 2) generated by 5-Hz frequency modulation of the radiofrequency field coupled with phase-sensitive detection. Curve C is a derivative ENDOR signal with H_0 at a parallel field (f); curves D and E are at a perpendicular field (g) but at two different microwave frequencies, 9.25 and 8.65 GHz, respectively.

As shown in Fig. 2, with the magnetic field set at any position the ENDOR patterns are essentially symmetrical about ν_p; the relatively lower signal strengths of low-frequency resonances (for example, ref. 31), can account for the asymmetry in intensities. In addition, the pattern shifts the predicted amount to lower frequency (≈0.9 MHz) when the microwave frequency is decreased 9.25 to 8.65 GHz (curves D and E), as observed most clearly in the more intense high-frequency half of the spectrum. Thus, we conclude that the ENDOR signals arise exclusively from protons.

Two distinct groups of proton ENDOR signals may be discerned in Fig. 2; one appears to arise from proton sets with similar coupling constants 1 MHz $\lesssim$ A $\lesssim$ 4 MHz; the other is from sets with 12 MHz $\lesssim$ A $\lesssim$ 24 MHz. The signals with small couplings are weaker than the others. This probably occurs in part because fewer protons contribute to the former signals and in part for well-understood reasons involving the finite width of the individual spin packets (32). Finally, the minimal differences between spectrum pairs taken at parallel and perpendicular field positions (Fig. 2, curves A and B and curves C and D) are important in considering the identity of the radical site, as discussed below.

Our experience with the ENDOR apparatus we use has been that ^{14}N ENDOR is more readily observed than resolved proton ENDOR such as seen in Fig. 2; indeed, our measurements of the enzyme's resting, ferric state give strong ^{14}N ENDOR over the region ≈2 to 10 MHz with H_0 set at $g_\parallel = 2$, and ≈7 to 18 MHz with H_0 set at $g_\perp = 6$ (unpublished data). The absence of ^{14}N signals in ES thus indicates that the free-radical site in ES has no appreciable spin density on nitrogen.

Analysis. As noted above, the g values are unlike those of π radicals. The apparent absence of spin density on nitrogen further argues against identifying the ES signal with tryptophanyl or histidyl radicals. We have checked this argument with molecular orbital calculations, using the convenient and highly reliable Hückel–McLachlan technique (17). The π-electron spin-density on the nitrogen of tryptophanyl cation is $\rho_N^\pi \approx 0.04$, which corresponds to ^{14}N hfs tensor values of ≈(1.1, 1.1, 6.7) MHz (ref. 14 and unpublished data); the third tensor component is associated with the normal to the molecular

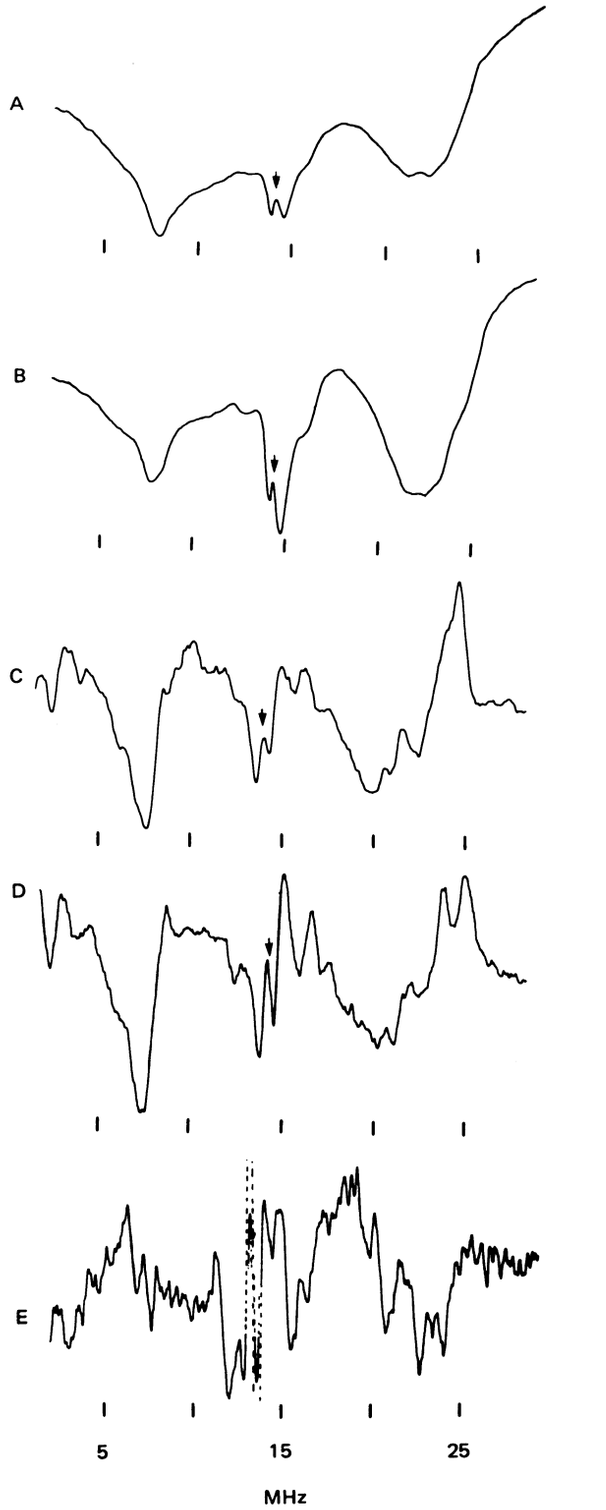

FIG. 2. ENDOR spectra of ES at 2 K in the range 2 to 30 MHz. Curves A and B are absorption presentation spectra (observed as a signal decrease); curves C, D, and E are derivative presentation spectra. Curves: A, field position f (Fig. 1), 9.25 GHz; B, position g, 9.25 GHz; C, position f, 9.25 GHz; D, position g, 9.25 GHz; E, position g (with instrumentally reserved derivative phasing), 8.65 GHz. Arrows indicate ν_p, the free proton frequency. Note that scales differ slightly between spectra.

plane and is assumed to correspond to $g_{\|}$. Taking as reasonable the quadrupole tensor values for pyrrole (33), computer simulations show not only that ^{14}N ENDOR should be seen in the frequency region of Fig. 2 but also that the pattern should change sharply between field positions f and g, contrary to observation (compare curves A to B and C to D in Fig. 2). Similar arguments hold for the histidyl radical.

The magnitudes of the proton couplings also indicate that the ES radical site is not a planar aromatic π radical. The ENDOR spectrum of a histidyl radical is known, and both the ring (α) and methylene (β) protons exhibit hfs couplings far too large to correspond with those observed for ES (34). ENDOR results for tyrosyl show that the α-proton couplings are within the range of values for ES but that the β-couplings would likely be larger (20).

The hfs tensors for tryptophanyl can also be estimated by using the π-spin densities calculated for ring carbon atoms (ρ_i^{π}) and the known proportionality between spin density and proton hfs (14). By this means we find that only one tryptophanyl ring proton should have an hfs tensor element in the range 12–22 MHz, although the ENDOR spectrum of ES shows that there must be a number of such couplings. The exception is H(2) which has an intermediate element close to these values ($\approx$25 MHz) but whose largest element, $\approx$35–40 MHz, is larger than any observed. Moreover, considerations of geometry indicate that one β-proton must have a coupling $A > 27$ MHz, again larger than any observed. The minimal difference between the proton ENDOR spectra at parallel and perpendicular field positions (Fig. 2) provides a general and independent indication that the ES radical site does not involve the α-protons of an aromatic π system, because the α-proton hfs tensor is highly anisotropic whereas β-proton tensors are much less so (14). Thus, a π-radical site is not in accord with the g value or with the ENDOR spectra of ES.

It was noted above that, although peroxy radicals have g values comparable to those of ES, they are unlikely on chemical grounds. The rich proton ENDOR of ES also would not be expected for such a site. In addition three sulfur-containing radicals were ruled out above on chemical grounds [RS, $(RSSR)^+$, and (R_2SSR)].

A dimeric thioether radical cation, $(R_2SSR_2)^+$, could be formed from two methionines by the loss of an electron. Models for such a dimer are of two kinds. In one the electron is largely localized on one sulfur (27); in the other it is equally shared (26). In both cases the average g value (2.01–2.02) is reported to be similar to, although slightly less than, that of ES (2.022). However, the g and hfs tensors of a dimer would undoubtedly depend on its geometry. The temperature and solvent dependence of the EPR signal of ES gives evidence that the radical is indeed sensitive to low-energy motions. Thus, the discrepancy in g values between ES and the models appears to be acceptably small.

All proton hyperfine couplings for a thioether radical, whether dimeric or monomeric, would be of the β type. Solution EPR studies of $(R_2SSR_2)^+$ radicals (26) and a single crystal study of γ-irradiated thiodiglycolic acid (35) both indicate that protons β to a spin-density bearing divalent sulfur have virtually isotropic hfs constants given by the relationship

$$A_{\beta} = B \cos^2 \Theta \rho_s^{\pi} \qquad [3]$$

in which ρ_s^{π} is the π-spin density on sulfur and θ is the dihedral angle between the z direction (normal to the C—S—C plane) and the C—H_{β} bond. The proportionality constant is calculated to be $B \approx 75$ MHz from the solution study and 63 MHz from the crystal measurements. In the latter work it was also suggested that B varies with conformation, supporting the above argument regarding g values.

A value for B of 60–70 MHz, or even substantially lower, rules out a dimer with the electron largely on a single sulfur ($\rho_{s_1}^{\pi} \approx 1$; $\rho_{s_2}^{\pi} \approx 0$). For example, the maximum β-proton isotropic couplings would have their lowest value, and thus the ENDOR spectrum would have its minimal breadth, if one of the methyl protons on the spin-bearing methionine lay near the C—S—C plane, placing the other two at roughly equal angles ($\theta \approx \pi/6$) with respect to the normal to this plane—namely, to the π orbital—and if $\theta > \pi/6$ for both methylene protons. Taking $B \approx 63$ MHz or even using a slightly decreased coupling parameter of $\approx$50 MHz (see below), such conformations would give $A \approx$ 47–38 MHz for the out-of-plane ($\theta = \pi/6$) methyl protons, producing an ENDOR pattern far different and far broader than that observed for ES.

Like the unsymmetrical dimer, a monomeric methionyl cation has $\rho_s^{\pi} \approx 1$. It is also ruled out by the identical arguments of isotropic coupling magnitudes and spectrum breadth. Indeed, because of the small isotropic proton hfs ($\approx$20 MHz) observed in irradiated methionine crystals (see ref. 36), it is clear that the species studied actually are the dimers, showing that a monomer $(RSR)^+$ cation radical is unstable with respect to dimerization with a nearby neutral R—S—R (37).

In contrast, a cation-radical dimer in which the sulfurs from two methionines share the spin density ($\rho_{s_1}^{\pi} \approx \rho_{s_2}^{\pi} \approx 1/2$) fits the available data. Such dimers have optical spectra (36, 38) similar to the spectrum of the ES radical. Considering hyperfine couplings, for tunneling or rotating methyl groups, the maximal coupling, $\approx B/4 \approx$ 16–19 MHz, is within the range seen for ES. If both methionines adopt the static conformation considered above, for $B \approx 63$ MHz, Eq. 3 predicts that the largest isotropic couplings for the dimer would be $A \approx 23$ MHz, and therefore the breadth of the ENDOR spectrum would be comparable to that of ES. In addition, the nearly in-plane ($\theta \approx \pi/2$) protons from the two methyls, and possibly also protons from the methylenes, would account for the resonances with small hfs. If a slightly decreased but still reasonable value of $B \approx 50$ MHz is used, the maximal isotropic coupling for these conformations becomes $A \approx 19$ MHz. Such a value is probably more attractive because it provides for a contribution to the spectrum breadth from the small anisotropic couplings of the β protons (14, 36). Finally, although many of the favorable features of $(R_2SSR_2)^+$ would be shared by an $(R_2SNR_3)^+$, if the electron is distributed roughly equally between N, say from histidine, and S (28), the absence of ^{14}N ENDOR diminishes this possibility.

A detailed interpretation of the ES proton ENDOR powder spectra in terms of the precise structure of a methionine-dimer cation radical would be exceedingly difficult to achieve, because one would have to take into account possible variations in B, differences in conformation between the two halves of the dimer, and departures from an idealized conformation as well as the possibility of multiple conformations. The small β-proton anisotropy probably accounts for the modest variation in the ES ENDOR spectrum as H_0 is set to different portions of the EPR spectrum (Fig. 2), but it also could result in each proton or proton set giving rise to one to three pairs of ENDOR features. Nevertheless, the $(R_2SSR_2)^+$ radical cation with shared electron appears to provide a plausible identification for the radical site of ES.

CONCLUSION

The combined EPR and ENDOR data for ES are inconsistent with previously proposed structures for the free radical site. In particular, the present results do not conform to an aromatic amino acid cation radical, despite the apparent support for such

a species by recent x-ray diffraction studies of ferric cytochrome *c* peroxide which locate a tryptophan in close proximity to the heme (11).

Instead, we have proposed[†‡] that the radical is sulfur-based and associated with a novel type of redox center in which the charge is shared between several side chains. The best available model is a dimeric cation radical formed from two methionines: $(R_2SSR_2)^+$. It is of interest, therefore, that the protein now has been shown to have at least one methionine in proximity to the heme, in a position which also offers potential for interaction with the proximal histidine (T. Poulos, personal communication).

The authors are grateful to Dr. T. Poulos for communicating results from the x-ray crystallographic studies of the enzyme and to Prof. A. L. Allred for use of the molecular orbital program. This work was supported by grants from the National Institutes of Health to B.M.H. (HL-13531) and E.M. (GM-19121), and from the National Science Foundation to B.M.H. (BMS-00478). The measurements were carried out in the magnetic resonance facility of Northwestern University's Materials Research Center, supported in part under the National Science Foundation NSF-MRL program (Grant DMR76-80847).

† Brown, T. G., Roberts, J. E., Hoffman, B. M., Kang, C. H., & Margoliash, E. (1979) *International Symposium on Magnetic Resonance in Chemistry, Biology, and Physics, June 24–28*, p. 29 (abstr.).

‡ Brown, T. G., Roberts, J., Hoffman, B. M., Kang, C. H. & Margoliash, E. (1979) *Abstracts of the XIth International Congress on Biochemistry*, p. 429 (abstr. no. 06-1-R42).

1. Altschul, A. M., Abrams, R. & Hogness, T. R. (1940) *J. Biol. Chem.* **136,** 777–794.
2. Yonetani, T. (1965) *J. Biol. Chem.* **240,** 4509–4514.
3. Coulson, A. F. W., Erman, J. E. & Yonetani, T. (1971) *J. Biol. Chem.* **246,** 917–924.
4. Yonetani, T. (1970) *Adv. Enzymol.* **33,** 309–335.
5. Chance, B. (1951) *Adv. Enzymol.* **12,** 153–190.
6. Lang, G., Spartalian, K. & Yonetani, T. (1976) *Biochim. Biophys. Acta* **451,** 250–258.
7. Iizuka, T., Kotani, M. & Yonetani, T. (1968) *Biochim. Biophys. Acta* **167,** 257–267.
8. Yonetani, T., Schleyer, H. & Ehrenberg, A. (1966) *J. Biol. Chem.* **241,** 3240–3243.
9. Wittenberg, B. A., Kampa, L., Wittenberg, J. B., Blumberg, W. E. & Peisach, J. (1968) *J. Biol. Chem.* **243,** 1863–1870.
10. Coulson, A. F. W. & Yonetani, T. (1972) *Biochem. Biophys. Res. Commun.* **49,** 391–398.
11. Poulos, T. L., Freer, S. T., Alden, R. A., Xuong, N. H., Edwards, S. L., Hamlin, R. C. & Kraut, J. (1978) *J. Biol. Chem.* **253,** 3730–3735.
12. Peisach, J., Blumberg, W. E., Wittenberg, B. A. & Wittenberg, J. B. (1968) *J. Biol. Chem.* **243,** 1871–1880.
13. Abragam, A. & Bleaney, B. (1970) *Electron Paramagnetic Resonance of Transition Ions* (Clarendon, Oxford).
14. Carrington, A. & McLachlan, A. D. (1967) *Introduction to Magnetic Resonance* (Harper & Row, New York).
15. Nelson, C. E., Sitzman, E. V., Kang, C. H. & Margoliash, E. (1977) *Anal. Biochem.* **83,** 622–631.
16. Brown, T. G. & Hoffman, B. M. (1980) *Mol. Phys.*, in press.
17. McLachlan, A. D. (1960) *Mol. Phys.* **3,** 233–252.
18. Feher, G. & Isaacson, R. A. (1972) *J. Mag. Reson.* **7,** 111–114.
19. Atherton, N. M. & Day, B. (1975) *Mol. Phys.* **29,** 325–338.
20. Box, H. C., Budzinski, E. E. & Freund, H. G. (1974) *J. Chem. Phys.* **61,** 2221–2226.
21. Allendorfer, R. D. (1974) *Chem. Phys. Lett.* **12,** 172–174.
22. McConnell, H. M. & Robertson, R. E. (1957) *J. Phys. Chem.* **61,** 1018–1019.
23. Schulz, C. W. Devaney, P. W., Winkler, H., DeBrunner, P. G., Doan, N., Chiang, R., Rutter, R. & Hager, L. (1979) *FEBS Lett.* **103,** 102–105.
24. Coulson, A. F. W. & Yonetani, T. (1975) *Biochemistry* **14,** 2389–2396.
25. Kou, W. W. H. & Box, H. C. (1976) *J. Chem. Phys.* **64,** 3060–3062.
26. Gilbert, B. C., Hogdeman, D. K. C. & Norman, R. O. C. (1973) *J. Chem. Soc. Perkin Trans. II* 1748–1752.
27. Musker, W. K. & Wolford, T. L. (1976) *J. Am. Chem. Soc.* **98,** 3055–3056.
28. Musker, W. K., Hirsehon, A. S. & Doi, J. T. (1978) *J. Am. Chem. Soc.* **100,** 7754–7756.
29. Rist, G. H. & Hyde, J. S. (1970) *J. Chem. Phys.* **52,** 4633–4643.
30. Brown, T. G., Roberts, J. E. & Hoffman, B. M. (1980) *J. Am. Chem. Soc.*, in press.
31. Davies, E. R. & Reddy, T. R. (1970) *Phys. Lett.* **31A,** 398–399.
32. Allendorfer, R. D. & Maki, A. H. (1970) *J. Magn. Reson.* **3,** 396–410.
33. Nygaard, L., Nielsen, J. T., Kirchheimer, J., Maltesen, G., Rastrup-Andersen, J. & Sorensen, G. O. (1960) *J. Mol. Struct.* **3,** 491–506.
34. Ngo, F. Q.-h., Budzinski, E. E. & Box, H. C. (1974) *J. Chem. Phys.* **60,** 3373–3377.
35. Wells, J. E. & Budzinski, E. E. (1973) *J. Chem. Phys.* **59,** 5211–5212.
36. Komimani, S. (1972) *J. Phys. Chem.* **76,** 1729–1733.
37. Bonifacic, M., Möckel, H., Bahnemann, D. & Asmus, K.-D. (1979 *J. Chem. Soc. Dalton Trans.* 675–685.
38. Asmus, K.-D., Bahnemann, D., Fischer, Ch.-H. & Veltwisch, D. (1979) *J. Am. Chem. Soc.* **101,** 5322–5329.